



Effects of Laminar Boundary Layer Control by Suction of a Stationary and Compressible Flow Around a Two-Dimensional Profile

Azzeddine Nahoui ^{a,*}, Zakaria Haddad ^a, Khalil Zerari ^b

^a *Laboratory LPCM, Faculty of Sciences, University of M'Sila, PO Box 166 Ichebilia, 28000 M'Sila, Algeria*

^b *Department of mechanical engineering and Electromechanical Institute of Science Engineering, Center University of Abdelhafid Boussouf, Mila, Algeria*

ARTICLE INFO

Article history:

Received September 02, 2025

Accepted October 06, 2025

Available online Oct 19, 2025

Published November 06, 2025

Keywords:

Laminar boundary layer,

Suction,

Control parameters.

ABSTRACT

Reducing aircraft energy consumption is a major challenge for aerodynamics specialists. This consumption is closely linked to the drag force. Drag has always hampered the smooth movement of the aircraft. To solve this problem, numerous theoretical and experimental studies have been conducted to eliminate or reduce the negative effects of drag. Knowing that the friction due to the turbulent boundary layer is much higher than that due to the laminar boundary layer, this generates greater energy consumption and, consequently, a degradation of aerodynamic performance. Much research has been conducted to ensure the persistence of the laminar layer while pushing the onset of the turbulent boundary layer towards the trailing edge, which also allows for greater laminarity. Controlling the laminar boundary layer by suction makes it possible to accelerate the tired particles of the boundary layer with reduced wall friction. This study aims to better understand and optimize the laminar boundary layer control parameters, angle, speed, and control range. The results obtained by numerical simulation allowed a gain of more than 10%.

1. INTRODUCTION

Reducing the strength devouring of an airplane by lowering the frictional drag provoked for one encircling flow has continually happened an important challenge for aerodynamicists (Kourta and Mazellier, 2011; Laure, 2014; Azim et al, 2015; Jahanmiri, 2010; Radespie et al, 2016; Yousefi and Saleh, 2014; Kucuk, 2015; Yousefi et al., 2013). To realize this aim, differing orders are second-hand, containing perimeter tier control. In the bound coating, the fluid is comparatively thin, and winding trade

* Corresponding author, E-mail address: azzeddine.nahoui@univ-msila.dz

the section, that produces frictional drag and deters the smooth campaign of the airplane (Schichiting, 1979). At the leading edge, the barrier coating is originally laminar accompanying nearly depressed resistance, and therefore enhances violent accompanying bigger disagreement towards the following edge. The aim is continually to hold the line tier as laminar as likely by mobile the change point of the perimeter coating backward (Venkatesha et al., 2020). There are differing border tier control methods, in the way that the influence pattern. This type of control has occurred deliberate for a lengthened occasion hesitantly (Venkatesha et al., 2020; Oluwasina et al., 2020; Baljit et al., 2017) and/or by mathematical substitution (Kianoosh et al., 2013; Beck et al., 2018; Cesar et al., 2018; Messing and Kloker, 2010; Wang and Lai, 2024). The greatest potential for threatening glossy drag display or take public the control of laminar flow by border level extract (Beck et al., 2018). This wonder is expressly advantageous in the aerospace district. Therefore, understanding the vehicle of BLS improves essential and the influence of eradication of liquid part and position, extract flow rate and evacuation of liquid traffic width on smooth act has survived checked by experiments and numerical studies (Ravindra et al., 2018). To overcome the misfortune of large extract needs, extract control for drag decline is advanced. Boundary level material opposition reduces drag by enduring the laminar skyline, therefore blocking the change, and accepting best laminar flow parishes (Ravindra et al., 2018). Boundary covering tangible fighting (BLS) still delays border covering schism, occurrence in a best CLmax (Ravindra et al., 2018). By communicable entirety in mind differing physical resistance characteristics in a way width, position, and extract joint, the schism putting off ability of an influence control is checked (Oluwasina et al., 2020). It was raising that inclusion imminent the forward edge can restrain the change and delay schism only when the inclusion field is spacious enough, but the flow physiognomy shame on account of eddy schism position further back (Wang and Lai, 2024). Suction well-known the following edge can raise flow acting by threatening the eddy portion in the back split of the arm and position further back domain, but it has little effect on the schism bubble and change (Wang and Lai, 2024). A chief transport ship plan uses awake edge level control by name disagreement, that reduces drag by acquiring the laminar line (Venkatesha et al., 2020). The influence of absorption points and position, inclusion flow rate, and inclusion dent width on smooth effectiveness is more significant (Venkatesha et al., 2020). Thus, forestalling the change and delaying bound level schism leads to a best lift cooperative and in an appropriate a main decrease in drag and pressure drops, apart from an increase in maximum lift, that increases the overall ship rendering (Venkatesha et al., 2020). Suction accompanying lower pressure at an outlined position leads the impediment level schism closer to the following edge of the writing (Azim et al., 2015). Choosing the right inclusion position reinforces glossy adeptness. Although multi-dent influence control can defeat drag much in a more wonderful category than unique-dent expulsion of liquid control, the tangible fighting dent position has a better effect on threatening pressure losses than the rubbing flow rate (Venkatesha et al., 2020). Direct analytical simulations are used to study the effects of individual-enclose incorporation ports on the clamour incident in three-dimensional laminar edge level flows following a favourable pressure slope (Ahmadi-Baloutaki et al., 2013). The results got by (Agriss et al., 2023) focus the cases place the blueprint capably reduces drag while reconstructing the lift-to-drag allotment. The results got by (Venkatesha et al., 2020) followed that a nonstop common rubbing can significantly increase the lift-to-drag allotment, what this percentage increases following evacuation of liquid force. The results captured by (Cesar et al., 2018) presented that a moderate flow absorption percentage can cause success partial flow laminarization, broadband decline of surface pressure ranges, and following edge sporadic roar. The present study attempts to devote effort to something surplus for laminar line level control by rubbing, about two together-dimensional NACA 0012 organ for Mach number ($M_\infty = 0.5$), Reynolds number ($Re = 3.10^5$), and zero angle of attack ($\alpha = 0^\circ$). The adding of material fighting angle, speed, and occasion, for better control by adjustment and the gear of these advanced limits on edge level breadth and difference joint.

2. BOUNDARY LAYER EQUATIONS AND SOLUTION ALGORITHM

2.1 Equations Governing the Boundary Layer

The physical problem is governed by nonlinear differential equations called Prandtl equations, which are :

$$\partial(\rho u)/\partial x + \partial(\rho v)/\partial y = 0 \quad (1)$$

$$\rho u (\partial u / \partial x) + \rho v (\partial v / \partial y) = \rho e U_e (dU_e / dx) + \partial(\partial x (\mu \partial u / \partial x)) \quad (2)$$

$$\rho u \partial H / \partial x + \rho v \partial H / \partial y = \partial[\mu/Pr(\partial H / \partial x) + \mu(1 - 1/Pr) \partial u / \partial x] / \partial x \quad (3)$$

Knowing that the total enthalpy H for an ideal gas is defined by

$$H = C_p T + u^2 / 2 \quad (4)$$

The external flow velocity U_e is also defined by

$$-dp/dx = \rho_e U_e (dU_e / dx) \quad (5)$$

With the following boundary conditions

$$u(x, 0) = 0, v(x, 0) = v_w \text{ and } H(x, 0) = H_w(x) \quad (6)$$

$$u(x, \delta) = U_e(x, \delta) \text{ and } H(x, \delta) = H_e(x) \quad (7)$$

To solve the Prandtl system of equations, we introduce the Falkner-Skan version, with a new dimensionless variable η and a running function ψ , defined by

$$d\eta = (\rho_e / \rho) dy, \psi = \sqrt{\rho_e \mu_e U_e x} f(x, y) \quad (8)$$

Thus, the velocity components become

$$\rho u = \partial \psi / \partial y, \rho v = -\partial \psi / \partial x \quad (9)$$

Defining the dimensionless total energy ratio S as,

$$S = H / H_e \quad (10)$$

The preceding system of partial differential equations becomes

$$(bf'')' + m_1 ff'' + m_2(c - f'f') = x(f'(\partial f' / \partial x) - f''(\partial f / \partial x)) \quad (11)$$

$$(bS' - df'f'') + m_1 ffS'' = x \left(f' \frac{\partial S}{\partial x} - S \frac{\partial f}{\partial x} \right) \quad (12)$$

With

$$\eta = \eta_e, f'(x, \eta_e) = 1, S(x, \eta_e) = 1 \quad (13)$$

The quantities b , C , c , d , e , m_1 and m_2 are defined such that

$$\partial(\rho u) / \partial x + \partial(\rho v) / \partial y = 0 \quad (14)$$

$$b = C = \frac{\rho u}{\rho_e \mu_e}, c = \frac{\rho_e}{\rho}, d = \frac{C \rho_e^2}{H_e} \left(1 - \frac{1}{Pr} \right) = 0 \quad (15)$$

$$e = \frac{C}{Pr}, m_2 = \frac{x}{U_e(x)} \frac{dU_e(x)}{dx}, m_1 = \frac{1}{2} \left(1 + m_2 + \frac{x}{\rho_e \mu_e} \frac{d(\rho_e \mu_e)}{dx} \right) \quad (16)$$

Thus, the physical problem is well modelled.

2.2 Resolution Algorithm

The discretization scheme used in this study is the Keller scheme, a stable scheme better suited to the study of the boundary layer. The solution of Prandtl's system of nonlinear partial differential equations using the Keller method can be achieved by following these steps:

- Reduce the order of the differential equations to first-order differential equations.
- Transform the resulting differential equations into algebraic equations by centred differences.
- Linearize the algebraic equations if they are nonlinear and put them into matrix form.
- Solve the resulting system of linear equations using the block elimination method.

3. RESULTS AND DISCUSSION

The free airflow (U_∞) is disrupted by the presence of the airfoil within it. Particles in direct contact with the airfoil wall are fatigued and, as a result, cause particles in the upper layers to separate. Air separation around the airfoil reduces the airfoil's aerodynamic performance. Therefore, avoiding separation by accelerating the fluid particles improves this performance. For a Mach number ($M_\infty = 0.5$), a zero angle of attack ($\alpha = 0^\circ$), and a Reynolds number ($R_\infty = 3.10^5$), a study of the ambient air around a two-dimensional symmetrical airfoil, NACA 0012, was conducted.



Fig 1. Symmetrical profile NACA 0012.

3.1 Effects of Suction Control

Suction control involves sucking in fluid particles slowed by wall-fluid friction and in direct contact with the wall. These slowed particles continue to accumulate on top of each other. Preventing the accumulation of fluid particles on the wall by suction accelerates the flow and thus delays boundary layer separation. Suction control is characterized by the suction angle (θ), the suction velocity relative to that of free air (U_w), and the suction length (extended x/c). These parameters are shown schematically in the figure below.

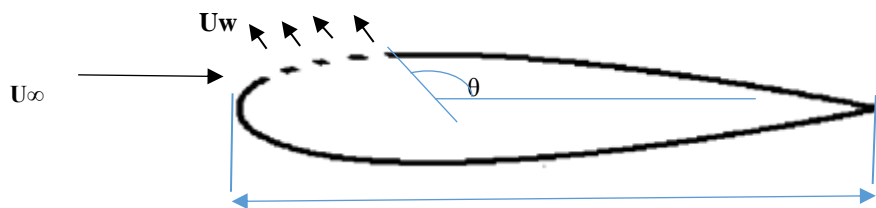


Fig 2. Diagram of suction control.

3.2 Validation of the Computational Code

By comparing the results of (Tousif et al., 2013) and those obtained by the developed computational code, we obtain very good agreement, which constitutes an initial validation of our code. At the leading edge, the pressure is maximum because all the kinetic energy is transformed into pressure energy following the complete cessation of the flow at this point; this is a stagnation point.

The flow then bypasses the profile, accelerating along the profile portion, then decelerates along the rear portion, producing a depression at the front and an overpressure at the rear up to the trailing edge.

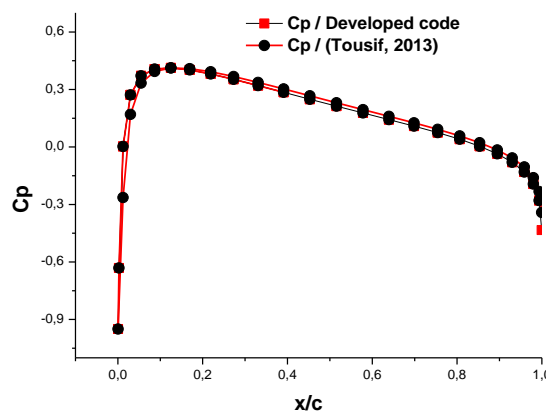


Fig 3. Comparison of pressure coefficients, NACA 0012, $\alpha = 0^\circ$.

3.3 Searching for Optimal Suction Control Values

3.3.1 Suction Angle

For arbitrarily chosen flow rate and suction range conditions, the effect of the suction angle is positive as soon as the value exceeds 75° . The higher the suction angle, the narrower the boundary layer separation point becomes towards the trailing edge. However, beyond 150° , the effect of the suction angle on the separation point remains virtually insensitive to any increase.

Therefore, there is no point in further increasing the suction angle. The 150° suction angle is oriented in the opposite direction of the flow; a complementary angle of 30° in the direction of the flow considered is therefore sufficient.

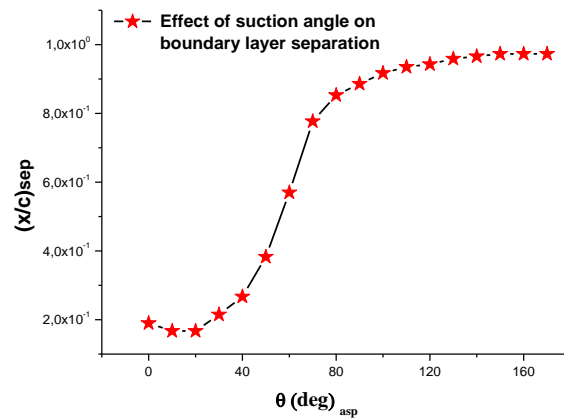


Fig 4. Effect of suction angle on the boundary layer separation, $x_{\text{extended}} = 10\%$.

3.3.2 Suction Flow

For arbitrarily chosen suction angle and width conditions, as shown below, the effect of suction flow on the boundary layer separation point is examined and plotted.

The flow rate is inversely proportional to the boundary layer separation point recession; therefore, there is no point in increasing the flow rate and settling for low flow rates. A flow rate of 10% or less has a positive effect on the boundary layer separation point recession (Fig. 5).

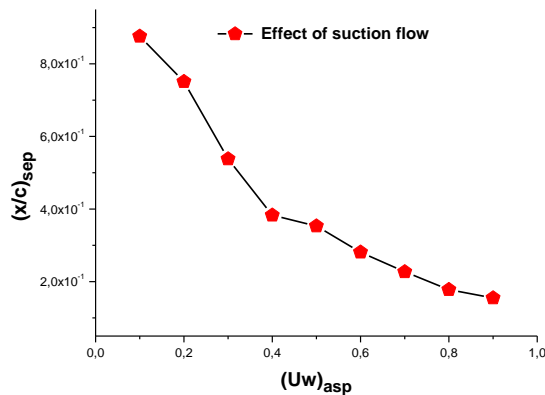


Fig 5. Effect of suction flow on the separation point, $x_{\text{extended}} = 10\%$, $\theta_{asp} = 75^\circ$.

3.3.3 Suction Range

For arbitrarily chosen flow rate and suction angle conditions, the effect of the suction range is positive as soon as the value exceeds 10%. The higher the suction range, the greater the displacement of the boundary layer separation point towards the trailing edge.

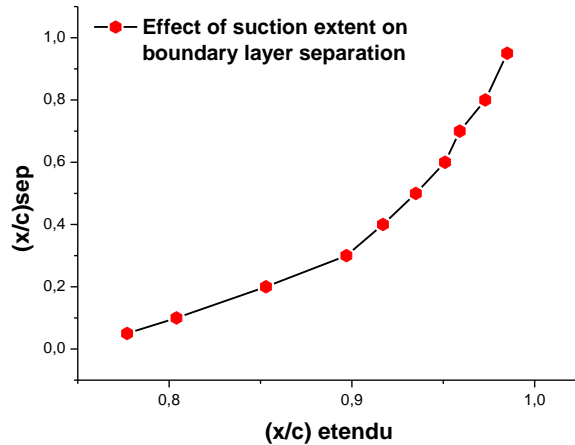


Fig 6. Effect of suction extent on separation point, $U_w = 10\%$, $\theta_{asp} = 70^\circ$.

3.4 Effect of Optimized Control Values

3.4.1 Effect of Optimized Values on Boundary Layer Thickness

The application of suction control extended the laminar zone and reduced the thickness of the laminar boundary layer by moving its separation point toward the trailing edge.

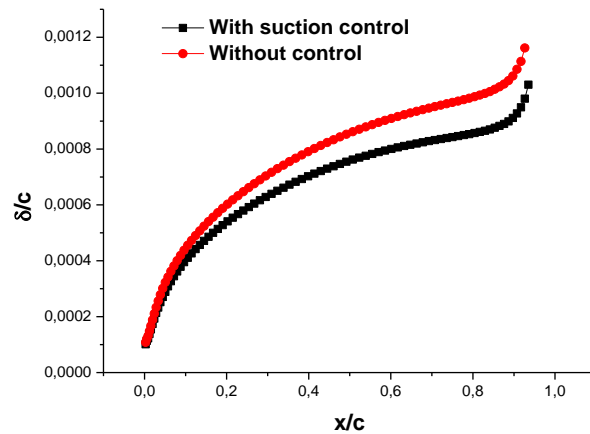


Fig 7. Effect of suction control on the boundary layer thickness, $x_{extended} = 5\%$, $U_w = 5\%$, $\theta_{asp} = 150^\circ$.

3.4.2 Effect of Optimized Values on the Local Friction Coefficient

The application of suction control delayed the separation of the laminar boundary layer, with a slight increase in the local friction coefficient compared to the case without control.

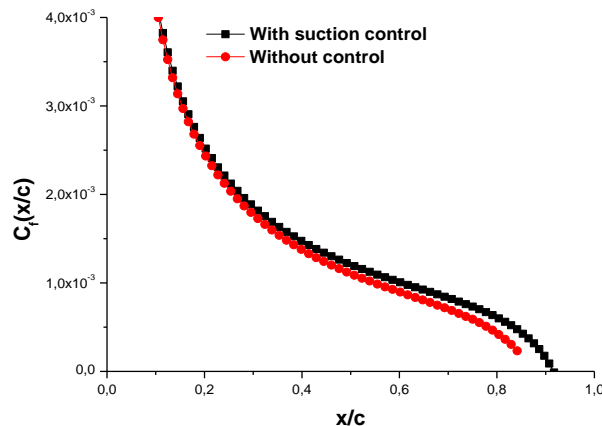


Fig 8. Effect of suction control on the local friction coefficient, $x_{\text{extended}} = 5\%$, $U_w = 5\%$, $\theta_{\text{asp}} = 150^\circ$.

CONCLUSION

Laminar boundary layer separation results in significant aerodynamic performance losses for the profile studied. This results in a minimization of lift and an increase in drag. The physical problem is addressed by the Prandtl mathematical model, and the mathematical solution is based on the Keller and Newton methods. The developed computer code allowed for the optimization of the suction control parameters. Indeed, with optimized values for a suction length of 5%, an angle of 150° , and a flow rate of 10%, the thickness of the laminar boundary layer was reduced, and the laminar zone was also enlarged. The applied suction control procedure resulted in:

- An extension of the laminar zone,
- A reduction in energy consumption,
- A reduction in noise,
- A significant 10% increase in laminarity.

ACKNOWLEDGMENTS

The authors warmly thank Professor Bahi Lakhdar of Frères Mentouri University for his advice, guidance, and explanations.

NOMENCLATURE

η	Dimensionless coordinate	ρ	Density [$\text{Kg} \cdot \text{m}^{-3}$]
c	Profile rope [m]	μ	Dynamic viscosity [$\text{Kg} \cdot \text{m}^{-1} \text{s}^{-1}$]
δ	Dimensionless thickness	Pr	Prandtl number
u	Axial velocity [m]	ψ	Fonction de courant []
v	Vertical velocity [m]	C_p	Specific heat [$\text{J} \cdot \text{kg}^{-1} \cdot \text{K}^{-1}$]
U_e	Potential flow velocity [m s^{-1}]	θ	Suction angle [$^\circ$]
p	Pression [$\text{N} \cdot \text{m}^{-2}$]	e	Extérieur
f	Current function	sep	Séparation
H	Enthalpy [$\text{J} \cdot \text{kg}^{-1}$]	asp	Aspiration
w	Wall		

REFERENCES

Agriss A., Agouzoul, M. and Ettaouil, A. (2023) Drag Reduction of a NACA Aerodynamic Airfoil: A Numerical Study, *Journal of Fluid Flow, Heat and Mass Transfer (JFFHMT)*; 10. DOI: 10.11159/jffhmt.2023.013

Ahmadi-Baloutaki, M., Sedaghat, A., Saghafian, M. and Badri, M. A. (2013) Control of Transition over Aerofoil Surfaces using Active Suction, *International Journal of Flow Control*; 5.

Azim, R., Hasana M. M. and Alib, M. (2015) Numerical investigation on the delay of boundary layer separation by suction for NACA 4162, *Procedia Engineering* 105, 109-191. doi: 10.1016/j.proeng.2015.05.013

Baljit, S., Saad, M. R., Nasib, A. Z., Sani, A., Rahman, M R A and Idris, A. C. (2017) Suction and Blowing Flow Control on Airfoil for Drag Reduction in Subsonic Flow, *Journal of Physics: Conf. Series* 914 012009 doi :10.1088/1748-6596/914/1/012009

Beck, N., Landa, T., Seitz, A., Boermans, L., Liu, Y. and Radespiel, R. (2018) Drag Reduction by Laminar Flow Control, *Energies*, 11, 252; doi:10.3200/en11010252. DOI 10.3200/en11010252

Cesar, L. M. Jawahar, H. K. and Azarpeyvand, M. (2018) Airfoil Trailing-edge Noise Reduction using Flow Suction, American Institute of Aeronautics and Astronautics. <https://doi.org/10.2514/6.2018-2814>

Jahanmiri, M. (2010) Active Flow Control: A review. *Research report* 2010:12. ISSN 1652-8549 Department of Applied Mechanics, Chalmers University of technology Goteborg, Sweden.

Kourta, A. and Mazellier, N. (2011). Amélioration de la portance aérodynamique d'un profil. *Revue de Mécanique Appliquée et Théorique*, 2011, 2 (5), pp.515-522. hal-00778522.

Laure, B. (2014) Étude et analyse des couches limites pour les écoulements turbulents, *Thèse*, CEMEF, France.

Liu, P. Q., Duan, H. S., Chen, J. Z. and He, Y. W. (2010) Numerical Study of Suction-Blowing Flow Control Technology for an Airfoil, *JOURNAL OF AIRCRAFT* Vol.47, No.1.

Messing, R. and Kloker, M. J. (2010) Investigation of suction for laminar flow control of three-dimensional boundary layers, *J. Fluid Mech.* (2010), Vol. 658, pp. 117–147. doi:10.1017/S0022112010001576

Oluwasina M. J., Saheed Adewale Adio, Adam Olatunji Muritala & Oluwasanmi Iyiola Alonge. (2020) The Suction Control Characteristics of Flow Separation on NACA 21192, *East African Journal of Engineering*, 2(1), 1-15. DOI: <https://doi.org/10.15284/eaje.2.1.121>

Radespie, R. (2016) Active flow control for high lift with steady blowing, *The Aeronautical Journal* January, Germany.

Ravindra Kulkarni, S., Rohit, B., Lokanatha, V., Lokesh, C. (2018) Understanding boundary layer suction and its effect on wings - A review. *IOP Conf. Ser.: Mater. Sci. Eng.* 376 012030. doi: 10.1088/1757-899X/376/1/012030

Schlichting, H. (1979) *Boundary layer theory*”, Seven Edition, Mc Graw-Hill Book Company.

Tousif, A., Tanjin Amin, Md., Rafiul Islam, S. M., Shabbir, A. (2013) Computational study of Flow around a NACA 0012 Wing Flapped at Different Flap Angles with Varying Mach number, *Global Journal of Research in engineering General engineering*, 13(4).

Venkatesha, S., Rakesh Vimal, S., Manigandan, S., and Gunasekar, P. (2020) Aerodynamic Investigation on Performance Enhancement of NACA 2162 Airfoil with Suction Assistance, *Vehicle Structures & Systems*, 12(1), 74-78. doi: 10.1873/ijvss.12.1.16

Wang, A. and Lai, H. (2024) Control of separated flow at low Reynolds number around NACA0012 airfoil by boundary layer suction, *Journal of Physics: Conf. Ser.* 2707 012122. DOI: 10.1088/1748-6596/2707/1/012122

Yousefi, K. and Saleh, R. (2014) The effects of trailing edge blowing on aerodynamic characteristics of the NACA 0012 airfoil and optimization of the blowing slot geometry, *Journal of theoretical and applied mechanics*, 52, 165-179. <https://api.semanticscholar.org/CorpusID:55680128>

Yousefi, K., Saleh, R. and Zahedi, P. (2013) Numerical investigation of suction and length of suction jet on aerodynamic characteristics of the NACA 0012 airfoil, *International Journal of Materials, Mechanics and Manufacturing*, 1(2). DOI: 10.7763/IJMM.2013.V1.13